Wood degradation by *Phellinus noxius*: ultrastructure and cytochemistry

M. Nicole, H. Chamberland, D. Rioux, X. Xixuan, R.A. Blanchette, J.P. Geiger, and G.B. Ouellette

Abstract: An ultrastructural and cytochemical investigation of the development of *Phellinus noxius*, a white-rot fungus, in wood chips of *Betula papyrifera* was done to gain insight into the cellular mechanisms of wood cell wall degradation. Extracellular sheaths and microhyphae were seen to be involved in wood colonization. Close association was observed between these fungal structures and wood cell walls at both early and advanced stages of wood alteration. Fungal sheaths were often seen deep inside host cell walls, sometimes enclosing residual wood fragments. Investigations using gold probes indicated the occurrence of β-1,3-glucans within the fungal sheaths, while β-1,4-glucans were detected only within the fungal septa. The positive reaction with the PATAg test revealed that polysaccharides such as β-1,6-glucans were important components of the sheath. Chitin, pectin, β-glucosides, galactosamine, mannose, sialic acid, fucose, and fimbrial proteins were not found to be present in the sheath. Our data suggest that extracellular sheaths and microphyphae produced by *P. noxius* during wood cell wall colonization play an important role in wood degradation.

Key words: cellulose, *Phellinus*, sheath, wood degradation.

Résumé : Une étude ultrastructurale et cytochimique a été entreprise in vitro dans le but d'élucider les mécanismes cellulaires de la dégradation du bois par *Phellinus noxius*, agent de pourriture blanche. La présence de matrices fongiques extracellulaires et de microhyphes a été observée durant la colonisation des cellules lignifiées. Dès les premiers stades de l'invasion, une association étroite existe entre ces structures et la paroi des cellules du bois et ce jusqu'à un stade avancé de l'altération des parois cellulaires. L'usage de sondes conjuguées à l'or colloïdal a montré que la matrice extracellulaire renfermait des β-1,3-glucanes, alors que les β-1,4-glucanes ne furent détectées que dans les septa des parois fongiques. Le test PATAg suggère que les β-1,6-glucanes sont des molécules importantes de la matrice. La chitine, la pectine, les β-glucosides, la galactosamine, le mannose, l'acide sialique, le fucose et les protéines de type fimbriae n'ont pas été détectés dans cette matrice. Nos résultats démontrent que les structures infectieuses de *P. noxius*, telles les matrices extracellulaires et les microhyphes, jouent un rôle prépondérant dans la dégradation du bois.

Mots clés : cellulose, *Phellinus*, dégradation du bois, matrice extracellulaire.

Introduction

Phellinus noxius (Corner) G.H. Cunningham (Aphyllophorales; Hymenochaetaceae) causes root diseases of numerous cultivated trees such as rubber, tea, coffee, and timber in tropical countries (Hodges 1984; Nandris et al. 1987; Thrower 1965). The most noticeable sign of infection is a dark brown, crusted mycelial sheath covering the roots and stem (Nandris et al. 1987). Infected roots fracture easily, showing large areas of decayed wood with small patches of white mycelium scattered throughout. Unlike *Rigidoporus lignosus* (Klotscht) Imaz., another tropical root-rotting fungus, *P. noxius* lacks rhizomorphs and thus spreads as ectotrophic mycelium across root contacts. Because fruiting bodies of *P. noxius* are seldom observed in tree plantations, the role of spores in the spread of disease remains unknown, although new infections by airborne basidiospores were reported (Hodges 1984).

Previous biochemical studies on wood decayed by *P. noxius* found that this fungus causes a typical white-pitted rot (Geiger et al. 1986*b*). This pathogen excretes a wide range of host cell wall degrading enzymes, but hydrolases were demonstrated to play a more important role in wood alteration than oxidases (Geiger et al. 1986*b*). In addition, microscopic observations in a time-course study of rubber seedlings infected with *P. noxius* revealed that root penetration and bark colonization were rapid, while xylem invasion was rather slow (Nicole et al. 1987). This

Received October 5, 1994. Revision received December 16, 1994. Accepted December 16, 1994.

M. Nicole,[1] **H. Chamberland, D. Rioux, X. Xixuan, and G.B. Ouellette.** Natural Resources Canada, Canadian Forest Service – Quebec Region, 1055, rue du P.E.P.S., B.P. 3800, Sainte-Foy, QC G1V 4C7, Canada.
R.A. Blanchette. University of Minnesota, Department of Plant Pathology, 495 Borlog Hall, 1991 Buford Circle, St. Paul, MN 55108, U.S.A.
J.P. Geiger. Institut français de recherche scientifique pour le développement en coopération, Laboratoire de phytopathologie, B.P. 5045, 34032 Montpellier, France.

[1] Author to whom all correspondence should be sent at the following address: Institut français de recherche scientifique pour le développement en coopération, Laboratoire de phytopathologie, B.P. 5045, 34032 Montpellier, France.

Table 1. Semi-quantitative estimation of positive cytochemical tests.

Probes	Sugar specificity	Wood cell wall	Mycelium		
			Sheath	Cell wall	Cytoplasm
β-1,4-Exoglucanase	β-1,4-Glucans	4	0	2[a]	0
β-1,3-Glucanase	β-1,3-Glucans	0	2	0	0
WGA + ovomucoid	*N*-Acetylglucosamine	2 to 3	0	2	0

NOTE: Rating scale: 0, no labeling, to 4, very intense labeling.
[a]In the septal wall.

work did not focus on the cellular mechanisms involved in cell wall degradation by *P. noxius*.

The present study was conducted to elucidate the degradation process of wood cells by means of ultrastructural and cytochemical techniques. Particular emphasis was placed on the structures produced by this fungus during wood decay and the role they may play in cell wall degradation.

Materials and methods

Fungal strains

Phellinus noxius (strain 2) was isolated from infected rubber tree roots in the Ivory Coast. It was routinely maintained on 2.5% malt agar (Difco, Detroit, Mich.) plates at 28°C.

Tissue processing for electron microscopy

Wood slices (0.5 × 0.2 × 0.1 cm) were taken from *Betula papyrifera*, autoclaved for 1 h at 110°C, and placed at the edge of 2-day-old *P. noxius* cultures on malt agar in Petri dishes. Autoclaved slices used as controls were placed on the medium without *P. noxius*. Cultures were incubated in the dark at 28°C and approximately 90% relative humidity. After 3, 6, and 11 days, control and decayed wood slices were prepared for transmission electron microscopy as described previously (Nicole et al. 1993). Briefly, wood fragments were fixed in 2.5% glutaraldehyde, rinsed in cacodylate buffer, and postfixed in 1% osmium tetroxide. After dehydration, samples were embedded in Epon and sectioned before examination with a Jeol 1200X transmission electron microscope. For scanning electron microscopy, samples were fixed with osmium tetroxide vapor for 24 h, coated with gold, and examined with a Cambridge S-150 microscope.

Cytochemistry

Polysaccharides were detected on thin sections by using the PATAg method (Thiéry 1967) modified as follows: periodic acid (60 min), thiocarbohydrazide (72 h), and 1% silver proteinate (30 min). Aniline blue (0.001 mg/mL in distilled water) was used on living fungal cells to visualize β-1,3-glucans. Observations were made with a Reichert Polyvar microscope using a BP 450- to 490-nm exciter filter combined with DS 510 and LP 515 barrier filters for blue illumination.

Lectins and enzymes conjugated to colloidal gold were used as probes for localizing different macromolecules in *P. noxius* cell walls and extracellular sheaths. Colloidal gold particles averaging 15 nm in diameter were prepared according to Frens (1973). The pH of the colloidal gold solution was adjusted to the isoelectric point of each enzyme and lectin used (Table 1). β-1,4-Glucans were localized using an exoglucanase complexed to gold at pH 9 (Nicole and Benhamou 1991*a*). RNase conjugated to gold at pH 9 (Bendayan 1981) was used for localizing RNA, and glucoside residues were localized using a β-glucosidase conjugated to gold at pH 9.3 (Bendayan and Benhamou 1987). β-1,3-Glucans were localized with β-1,3-glucanase purified from zymolyase 20T (Seikagaku Corporation, Tokyo) and conjugated to colloidal gold at pH 7.37. *N*-Acetylglucosamine, *N*-acetylgalactosamine, α-D-mannose and α-D-glucose, D-galactose, sialic acid, and α-L-fucose were localized using wheat germ agglutinin (WGA) followed by ovomucoid–gold at pH 4.95, *Helix pomatia* agglutinin (HpA) at pH 7.4, concanavalin A (ConA) at pH 8.0, *Ricinus communis* agglutinin (RcA) at pH 8.0, *Limax flavus* agglutinin (LfA) followed by fetuin–gold at pH 7.3, and *Ulex europaeus* (UeA) at pH 6.3 (Roth 1983; Roth et al. 1984), respectively.

The specificity of the different labelings was assessed by the following control tests: (*i*) incubation with gold-complexed protein to which was added the corresponding sugar molecule; β-1,4-glucans from barley for the exoglucanase–gold probe; RNA (Sigma, St. Louis, Mo.) for the RNase probe; D-glucose for the glucosidase–gold probe; laminarin for the β-1,3-glucanase; *N*-acetylgalactosamine for the HpA–gold complex; D-mannose for the ConA–gold complex, D-galactose for the RcA–gold complex, and α-L-fucose for the UeA–gold complex; (*ii*) incubation with WGA, previously adsorbed with *N*-acetylchitotriose, followed by incubation with the ovomucoid–gold complex; (*iii*) incubation with LfA, previously adsorbed with neuraminic acid (sialic acid) followed by incubation with the fetuin–gold complex.

Immunocytochemistry

Antiserum raised against fimbriae of *Ustilago violacea* was used to reveal the presence of fimbrial proteins in *P. noxius* sheaths as described by Benhamou et al. (1986). Specificity of labeling was assessed through the following control experiments performed on control or decayed samples: (*i*) incubation with antifimbria antiserum previously adsorbed with the antigen, (*ii*) incubation with preimmune rabbit serum instead of the primary antiserum, and (*iii*) omission of the primary antibody incubation step.

Monoclonal antibodies (JIM5) raised against unesterified epitopes of pectin were used to visualize molecules containing galacturonic acid over hyphal sheaths. Immunogold localization of pectin was performed as previously described by Knox et al. (1990). Briefly, sections were first incubated on

Table 2. Density of gold particles per square micrometre over the fungal cell and wood cell walls after incubation with the β-1,4-exoglucanase–gold complex for localizing β-1,4-glucans.

	Days after inoculation						
	0	3	6	11	χ^2	*P*	
Background	0.25±0.36	0.48±0.67	0.32±0.39	0.16±0.23	1.7	>0.1	(ns)
Mycelium	0.20±0.15	0.88±1.24	0.09±0.17	0.26±0.45	1.7	>0.1	(ns)
HCW 1[a]	125.25±12.05	52.35±37.78	35.29±28.23	27.53±14.30	6.9	<0.05	(s)
HCW 2[b]	129.17±9.58	94.78±43.77	70.40±24.05	59.09±17.70	1.2	<0.05	(s)

NOTE: Data are expressed as means of 8–15 fields. s, significant; ns, nonsignificant.
[a] Density over host cell walls (HCW) close to the fungal hyphae.
[b] Density over host cell wall (HCW) at a distance from the fungal hyphae.

a drop of primary antibodies for 2 h at 37°C and then on a drop of gold-labeled goat anti-rat antibodies for 30 min at 37°C.

General controls

In addition to the controls reported above, each gold probe was also used on other plant (tomato, pea) and fungal (*Ophiostoma ulmi*, *Fusarium* sp.) embedded material on which these probes were known to provide positive labeling.

Quantitation of labeling

To evaluate wood degradation after the use of the exoglucanase–gold probe, the density of labeling (*D*) over control and decayed wood was compared by determining the number of gold particles per square micrometre ± standard error. Areas were determined on scanned micrographs using Image, a picture processing shareware, loaded on a Macintosh SE 30 computer (Apple). Density of labeling was calculated as follows: $D = Ns/Sa$, where Ns is the number of gold particles and Sa is the surface area. Densities were determined by counting the number of gold particles over specified cell areas on 8–15 fields taken randomly from serial sections at a magnification of × 12 000 – 40 000. The average gold particle densities for healthy and infected tissues were compared using the Kruskal–Wallis rank test, which is based on a statistic distributed as chi-square with one degree of freedom. The value of the statistic and the corresponding *P* value are given in Table 2.

Results

Scanning electron microscopy of *P. noxius* during wood degradation

Three days after inoculation, wood chip surfaces colonized by *P. noxius* showed thick-walled septate hyphae that were frequently branched (Fig. 1A). Numerous hyphae were covered by apparently thin sheaths (Figs. 1A, 1B, 1C) that seemed to be closely connected to the surface (Figs. 1A, 1B). A more abundant mycelium with branched cluster hyphae (Fig. 1C) and unbranched thin-walled hyphae was observed 6 days after inoculation. Both types of hyphae sometimes produced spherical swollen vesicles (Fig. 1D). Eleven days after inoculation, wood chips were colonized by a dense mycelium (Fig. 1E) that displayed dendrohyphidialike elements (Figs. 1E, 1F). The trichocysts, routinely observed at this time, had numerous short projections arising from the main hypha (Fig. 1F). They were produced either by thick-walled hyphae on the wood chip surface or by hyphae located inside wood cells (Fig. 1F).

Transmission electron microscopy of wood degradation by *P. noxius*

A positive reaction for polysaccharide staining was recorded with the PATAg reaction over both the fungal cell wall and sheaths (data not shown). Labeling of sheaths was observed only after using a β-1,3-glucanase gold probe for localization of β-1,3-glucans (Table 1). In these experiments, gold particles were also seen over the fungal cell wall (Fig. 2A). The use of WGA followed by the ovomucoid–gold complex for the localization of *N*-acetylglucosamine resulted in a strong labeling of both thin and thick fungal cell walls (Figs. 2B, 2C, 2D; Table 1), whereas no significant labeling occurred over *P. noxius* sheath material (Fig. 2D). β-1,4-Glucans were detected only in the fungal septae that were evenly labeled (Fig. 2E; Table 1). Glucopyranoside, RNA, galactosamine, mannose, galactose, sialic acid, and fucose were not detected over the cell wall and sheath. Immunolocalization of pectinlike components as well as fimbrial proteins resulted in the absence of gold particles over fungal structures, including the extracellular material.

The intensity of wood degradation by *P. noxius* was estimated by means of an exoglucanase–gold complex that specifically binds to β-1,4-glucans of the free ends of cellulose fibrils. Quantitation of gold particles revealed that the density of labeling decreased with incubation time over infected wood cell walls both close to and away from the fungus (Table 2). Three and 6 days after inoculation, high standard errors indicated great variations in wood degradation.

Three days after inoculation, large portions of host cell walls were removed (Fig. 3A), although few hyphae were observed within the wood chips. Numerous hyphae, located at the wood surface, were surrounded by an extracellular sheath that appeared to be composed of a fibrillar material (Figs. 3B, 3C, 3D, 3E). At this time, a close association was seen between sheaths and wood degradation both on the wood surface (Fig. 3C) and inside cell walls (Figs. 3D, 3E). The reduction of gold labeling over host cell areas close to sheaths indicated that walls were degraded (Fig. 3D). Some cell wall portions at the wood surface were detached and surrounded by the hyphal sheath (Fig. 3C). Inside the cell walls of vessels or tracheids, sheaths were also closely associated with altered wall areas that

Fig. 1. Scanning electron microscopy. (A and B) Three days after inoculation, septate and branched hyphae (*h*) of *P. noxius* are noted over wood chips. Extracellular sheaths (*s*) are associated with the fungal hyphae and seem closely connected to the wood surface (arrows). (A, ×2000; B, ×2000). (C) Six days after inoculation, abundant mycelium with cluster of hyphae (arrow) cover the wood chip surface. There are both thick and thin hyphae and sheaths surround some of them. ×500. (D) Six days after inoculation a thin-walled hypha (*h*) shows a swollen spherical vesicle. ×2000. (E and F) Eleven days after inoculation, a dense mycelium contains dendrohyphidialike elements (arrows). In F, such an element arises from inside a wood cell (E, ×200; F, ×2000).

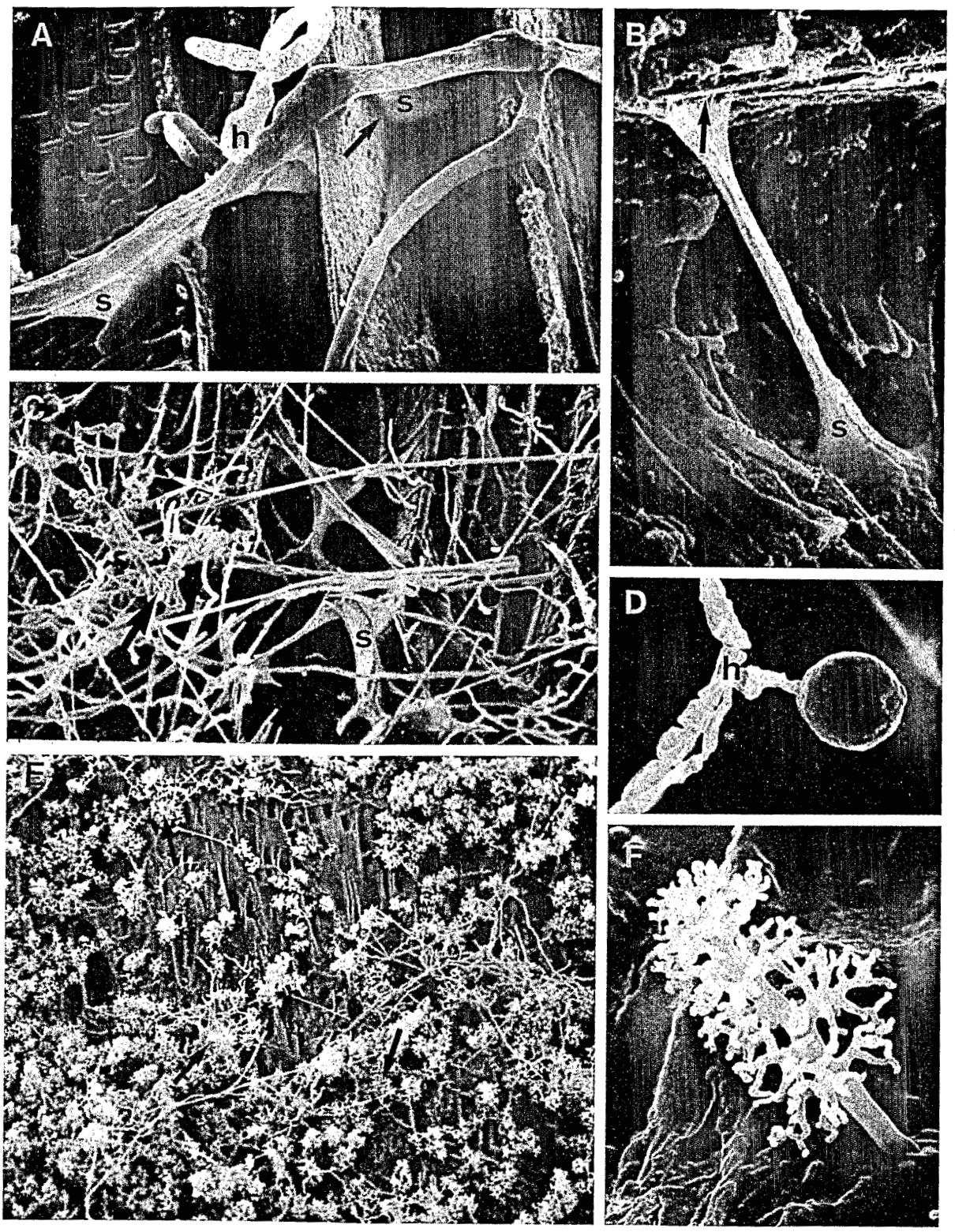

Fig. 2. Transmission electron microscopy (TEM) showing the cytochemistry of the fungal cell wall. (A, B, and C) Cytolocalization of *N*-acetylglucosamine residues by the WGA and ovomucoid–gold method. Gold particles are seen over both thin-walled (A and B, arrow) and thick-walled (A, double arrows, and C) hyphae (*h*). No labeling occurs over the fungal sheath (*s*). *c*, host cell. (A, × 24 000; B, × 15 600; C, × 17 000). (D) Cytolocalization of β-1,3-glucans by the β-1,3-glucanase–gold complex. The fungal cell wall (*w*) and sheath are evenly labeled, while no gold particles are seen in the fungal cell. × 28 000. (E) Cytolocalization of β-1,4-glucans by the β-1,4-exoglucanase–gold complex. The hyphal septum is partly labeled (arrow), while no gold particles are seen over the fungal cell wall (double arrow). × 32 000.

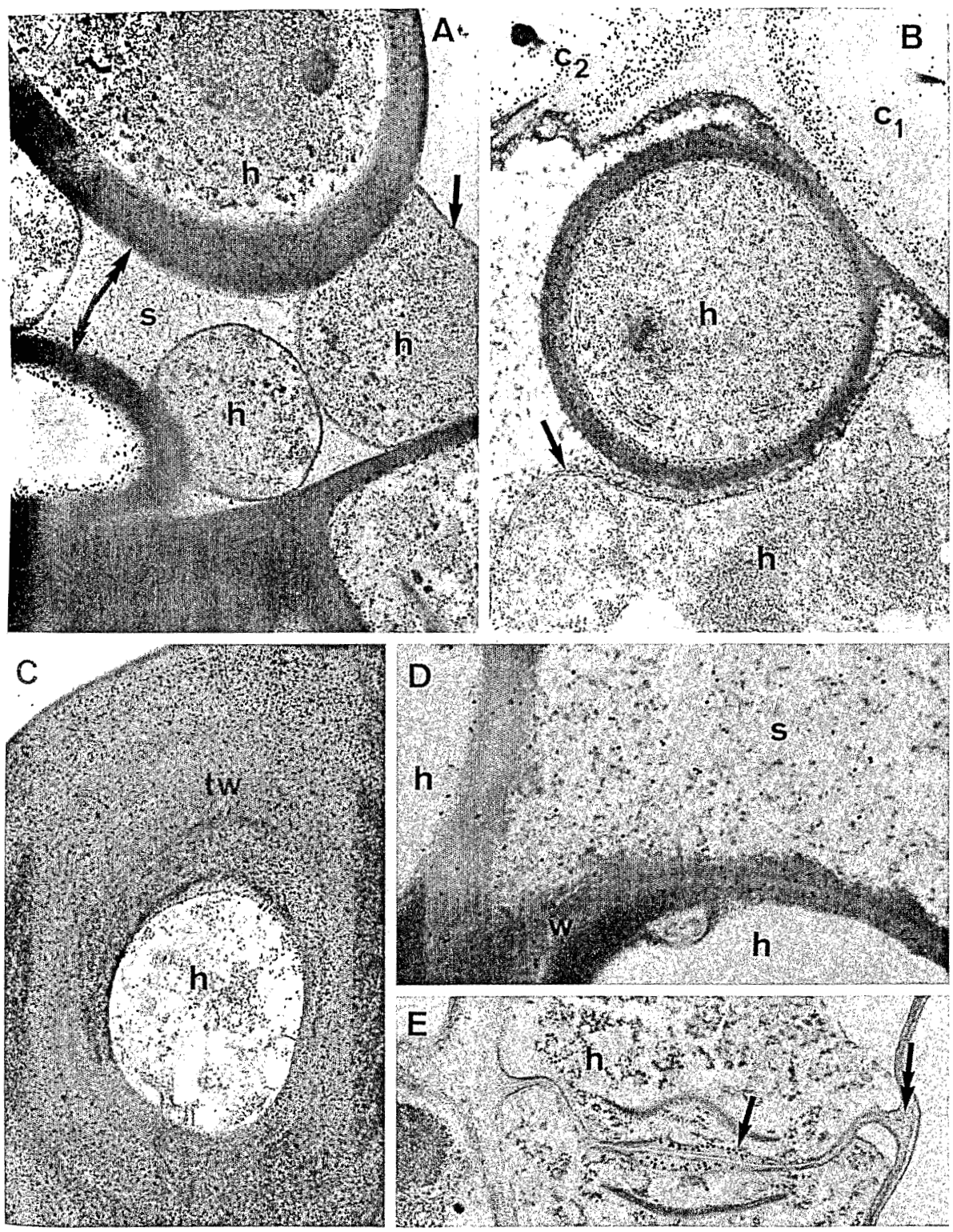

Fig. 3. TEM of wood degradation 3 days after inoculation with *P. noxius*. Cytolocalization of β-1,4-glucans in wood cell walls. (A) Large areas of host cell walls (arrows) are highly degraded; labeled portions of cell walls are seen in the cell lumen (arrowheads). ×8000. (B) The sheath (*s*) surrounding the hypha (*h*) consists of dense fibrils that are devoid of labeling × 37 500. (C) The dense sheath in contact with the hypha is closely associated with the eroded wood surface (arrows). An electron-dense material is seen (arrowheads) between a detached wall portion and the vessel cell wall. × 32 000. (D) A hypha is partly located within a highly degraded area of the wood cell wall (arrow). A small amount of label is seen over the fungal sheath that seems to be closely associated with the degraded cell walls. × 19 500. (E) The loosened fungal sheath present at the wood surface is associated with the eroded labeled wall (arrows). × 17 000. *cw*, wood cell wall.

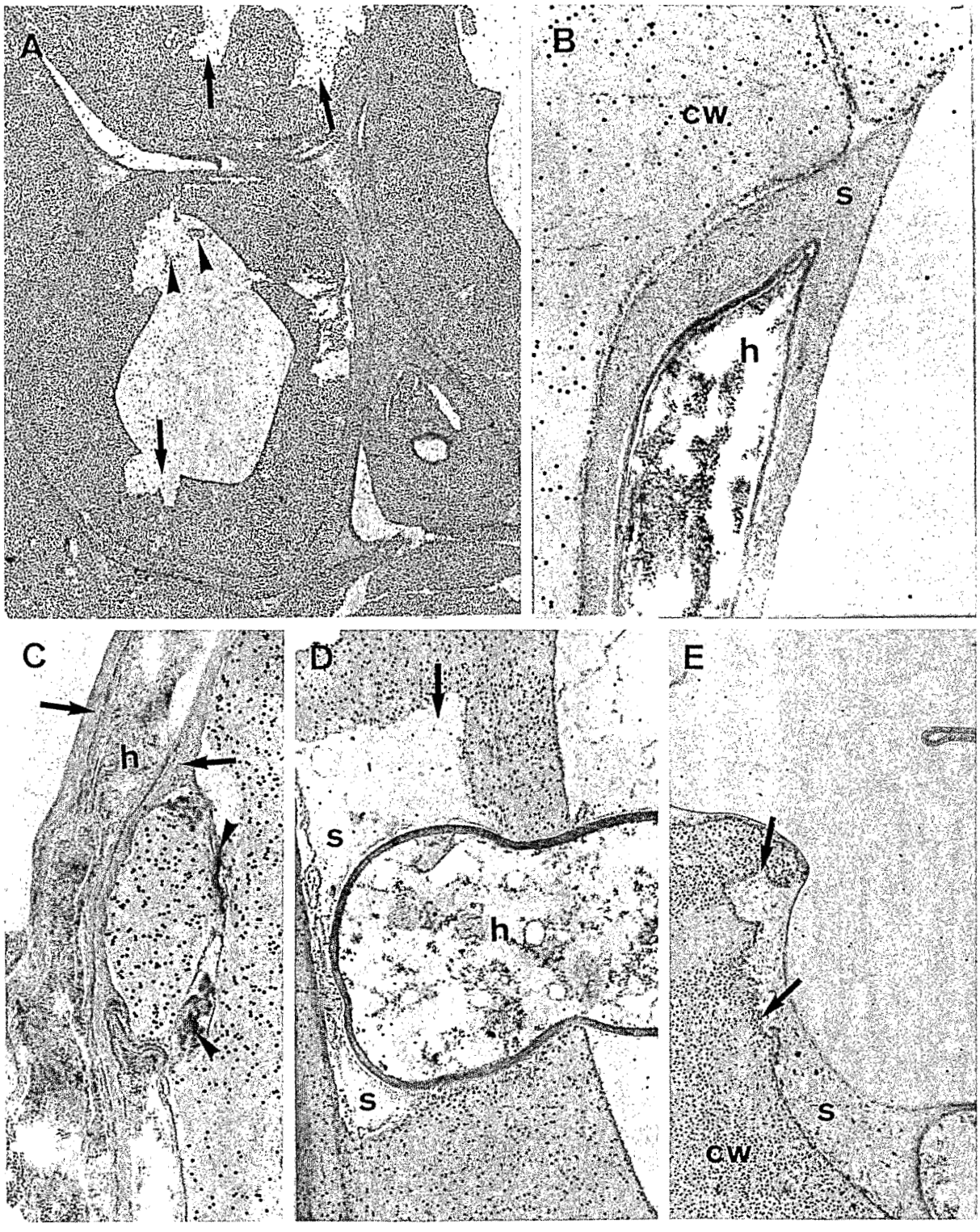

were devoid of significant labeling for β-1,4-exoglucans (Fig. 4A). Observation of wood sections also revealed that cell walls were penetrated by fine hyphae, or microhyphae, produced by lumen-colonizing mycelium of *P. noxius* (Figs. 4B, 4C, 4D, 4E). Digestion of secondary and primary walls was consistently observed in contact with microhyphae during fungal ingress into wood cells (Figs. 4C, 4D, 4E) and wall erosion resulted in channels displaying chiseled (Fig. 4C) or fibrillar edges (Fig. 4D). Also, electron-dense material that occurred in cavities close to the fungus likely resulted from degradation (Fig. 4E).

Six days after inoculation, fibrillar sheaths were always associated with degradation of wood residues (Fig. 5A). The fact that these fungal sheaths were devoid of gold particles after labeling for β-1,4-glucans and *N*-acetylglucosamine greatly facilitated observation of them within labeled wood cell walls (Figs. 5A, 5B, 6A). At this time of colonization, large portions of the extracellular fungal material were electron opaque. (Fig. 5C) and sometimes surrounded several hyphae that filled the vessel lumen (Fig. 5D). Observations of this electron-opaque material revealed that it established close connections between the fungal cell wall and the wood cell wall (Figs. 5D, 5E, 6A) and at times it also filled degraded wall areas (Figs. 5C, 6A, 6B, 6C). Microhyphae, with a diameter that ranged from 0.2 to 0.5 μm, were observed routinely within cell walls of infected wood at both 6 and 11 days after inoculation (Figs. 6D, 6E). A zone consisting of strands of material extending from the wood cell wall to the fungal cell was frequently present around microhyphae (Figs. 4D, 6D, 6E).

Examination of wood samples 11 days after inoculation revealed advanced stages of decay characterized by the presence of numerous cavities within tracheid cell walls (Fig. 7A). The degraded areas were devoid of any significant labeling after the use of the β-1,4-exoglucanase–gold probe. Most hyphae observed within wood cell walls displayed a thick and multilayered cell wall exhibiting alternating light and electron-opaque layers (Figs. 7B, 7C). Such hyphae could be seen tunneling within host cell walls, including the primary wall and the middle lamella (Figs. 6A, 7C). As observed with 6-day samples, a very close association between the electron-opaque sheath and degraded wall areas (Fig. 7D) was noted. In addition, strands of labeled wood fragments were distinguishable within the electron-dense material (Figs. 7B, 7C).

Discussion

This research was undertaken to better understand wood deterioration by the tropical white-rotting fungus *P. noxius*. Except for previous ultrastructural works on white-pocket rot caused by *Phellinus pini* (Blanchette 1980, 1982), cellular aspects of wood degradation by tropical *Phellinus* species are to our knowledge poorly documented. Scanning electron microscopic (SEM) observations of *P. noxius*-infected wood chips revealed that dendrohyphidiumlike elements, also called trichocysts (Adaskaveg et al. 1991), arising from hyphae during alteration of lignified cells, resemble those reported by Adaskaveg et al. (1991) on a newly described species, *Phellinus ralunensis* from Chile. These authors pointed out that other species of *Phellinus* have not displayed such structures.

Using probes conjugated to colloidal gold, transmission electron microscopy (TEM) provided information on cellular mechanisms of in vitro wood degradation by *P. noxius*. Quantitation of gold labeling after the use of an exoglucanase–gold probe unambiguously indicated that cellulose was strongly modified during wood cell colonization by the fungus. Both the primary and secondary walls, as well as the middle lamella, displayed severe damage, suggesting that polysaccharides and lignin were degraded, as reported previously for other *Phellinus* species (Blanchette 1980, 1982). Our observations are in accordance with previous biochemical studies that demonstrated the wide range of degrading enzymes secreted by *P. noxius* during wood degradation in planta as well as within sterilized wood fragments (Geiger et al. 1986*a*, 1986*b*). The decay caused by this pathogen probably results from high activity levels of hydrolases instead of oxidase enzymes (Geiger et al. 1986*a*, 1986*b*), as indicated by the important reduction of gold particle densities at 3 days after inculation (Table 2). Degradation patterns of wood chips close to, but particularly away from, the hyphae showed that the fungal degrading enzymes may diffuse within infected cells.

In this study, we reported the presence of β-1,4-glucans in hyphal septa of *P. noxius*, but we did not detect them in the walls or in the sheath. Although cellulose was demonstrated to be a structural component of oomycetes (Benhamou and Côté 1992; Wessels and Sietsma 1981) and of *Ophiostoma ulmi* (Benhamou et al. 1987), this is the first report of the occurrence of β-1,4-glucans in root-rotting fungi.

Our ultrastructural observations revealed that *P. noxius* produces both extracellular sheaths and microhyphae that appear to be involved in wood colonization and degradation. Sheaths, which are well-known structures occurring in many fungi (Benhamou and Ouellette 1987; Murmanis et al. 1984; Nicole et al. 1993, 1994), are known to contain β-1,3-glucans substituted with β-1,6-linked glucans. Cytolocalization of β-1,3-glucans and the positive PATAg staining within the sheath of *P. noxius* confirm previous findings on the chemical constitution of fungal sheaths (Nicole et al. 1994; Ruel and Joseleau 1991). In the present study, we also showed, by SEM and TEM, that with *P. noxius* the sheath is differentiated at the early stage of wood invasion and that it is present in degraded areas of both primary and secondary wall layers and the middle lamella. Recent immunolocalization studies of wood-degrading enzymes have provided evidence that fungal sheaths are directly involved in wood degradation (Blanchette et al. 1989; Gallagher and Evans 1990; Green et al. 1992; Nicole et al. 1993; Ruel and Joseleau 1991). Although such enzymes were not localized in the present study, the close association of *P. noxius* sheaths with altered wood cells and the occurrence of host cell wall fragments within the sheath strongly suggest that the extracellular fungal matrix produced by this fungus is involved in cell wall alteration.

Phellinus noxius also produces microhyphae that grow intramurally for appreciable distances in xylem cells. Within host walls, they were found to be associated with primary and secondary wall breakdown and alteration of the middle lamella. Microhyphae were first reported for soft rot and blue stain fungi (Liese and Schmid 1963), for the tree pathogen *O. ulmi* (Ouellette 1962), and then for the Ascomycotina (including Deuteromycotina) and Basidiomycotina (Corbett 1965; Peek et al. 1972; Zainal 1976; Murmanis et al. 1984). The most

Fig. 4. TEM of wood degradation 3 days after inoculation with *P. noxius*. Cytolocalization of β-1,4-glucans in wood cell walls. (A) A hypha (*h*) is localized within wood cell walls. (*cw*). Unlabeled portions of cell walls are seen in contact with the fungus (arrows). *s*, sheath. × 18 000. (B) A microhypha (*m*) has penetrated the secondary wall. Host wall degradation has occurred at the edges of the channel of penetration. × 24 000. (C, D, and E) Host cell wall penetrated by microhyphae displays various aspects of erosion resulting in chiseled (C) or fibrillar (D) channel edges (arrows). Electron-dense material (arrowheads) is observed between the microhypha and the degraded cell wall (E). (C, × 60 000; D, × 62 000; E, × 40 000).

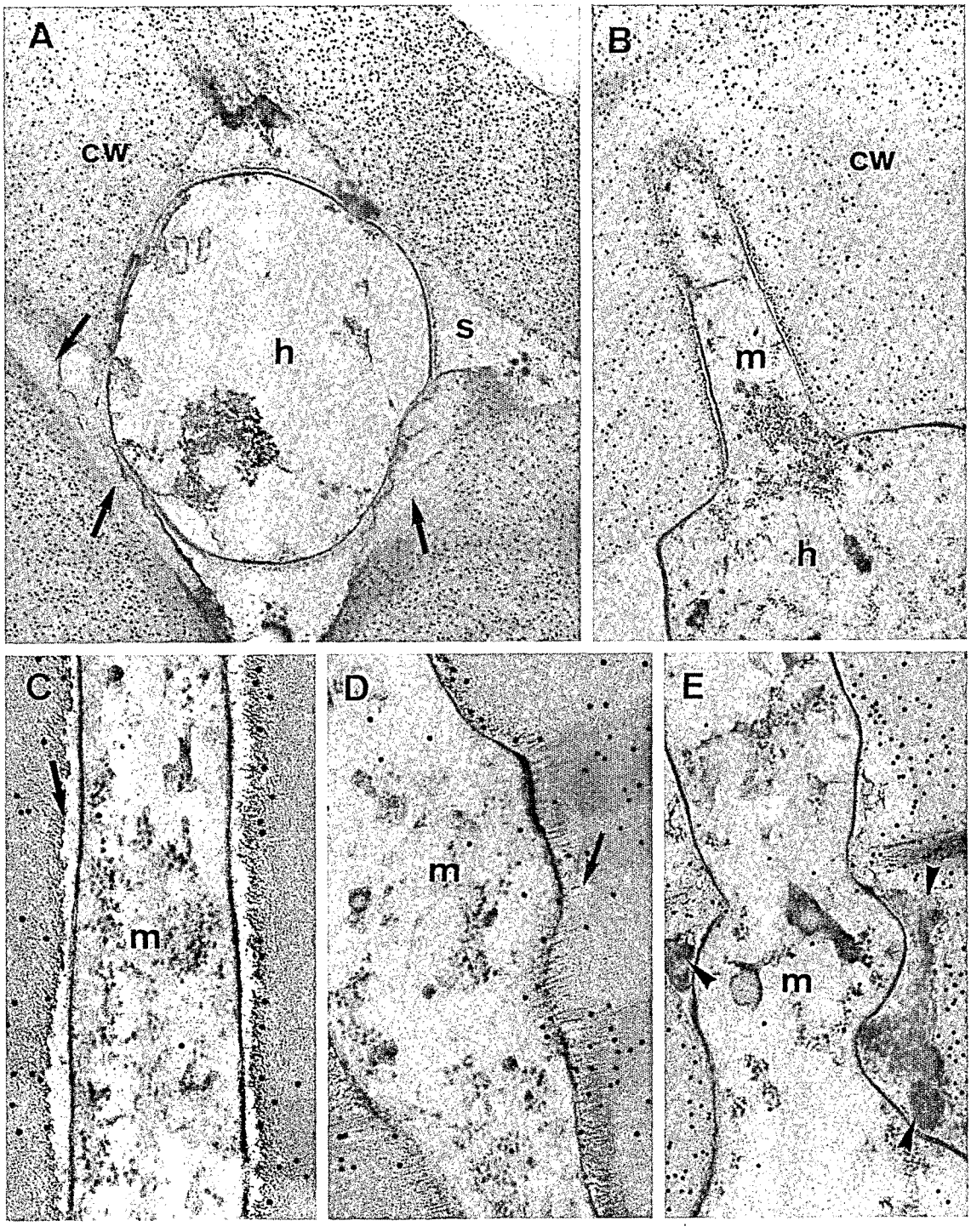

salient feature of microhyphae has been described by Hale and Eaton (1985*a*, 1985*b*, 1985*c*) for soft-rot fungi. These authors specified that microhyphae are formed predominantly within secondary cell wall layers of xylem in woody plants. Microhyphae produced by *P. noxius* were seen within the different cell wall elements, suggesting that they are able to

Fig. 5. TEM of wood degradation 6 days after inoculation with *P. noxius*. (A) Cytolocalization of *N*-acetylglucosamine residues. No gold particles are observed over the fibrillar fungal sheath associated with degraded cell wall areas (arrow). Portions of the host cell wall (*cw*) are noted within the sheath (arrowheads). × 24 000. (B–E) Cytolocalization of β-1,4-glucans in wood cell walls. (B) Unlabeled fibrillar sheath is observed within the labeled wood cell wall. × 28 000. (C) An electron-dense extracellular material lies between the hypha and the wood cell wall. A portion of the cell wall is detached from the main cell frame (arrows). × 48 000. (D) Several hyphae filling the lumen of a wood cell are surrounded by an electron-dense material. Dark areas are seen in the host cell wall close to a hypha (arrows). ×8000. (E) Enlargement of a portion of D. The electron-dense fungal extracellular material is closely associated with digested wood cell wall (arrows). × 60 000. *s*, fungal sheath; *h*, hypha.

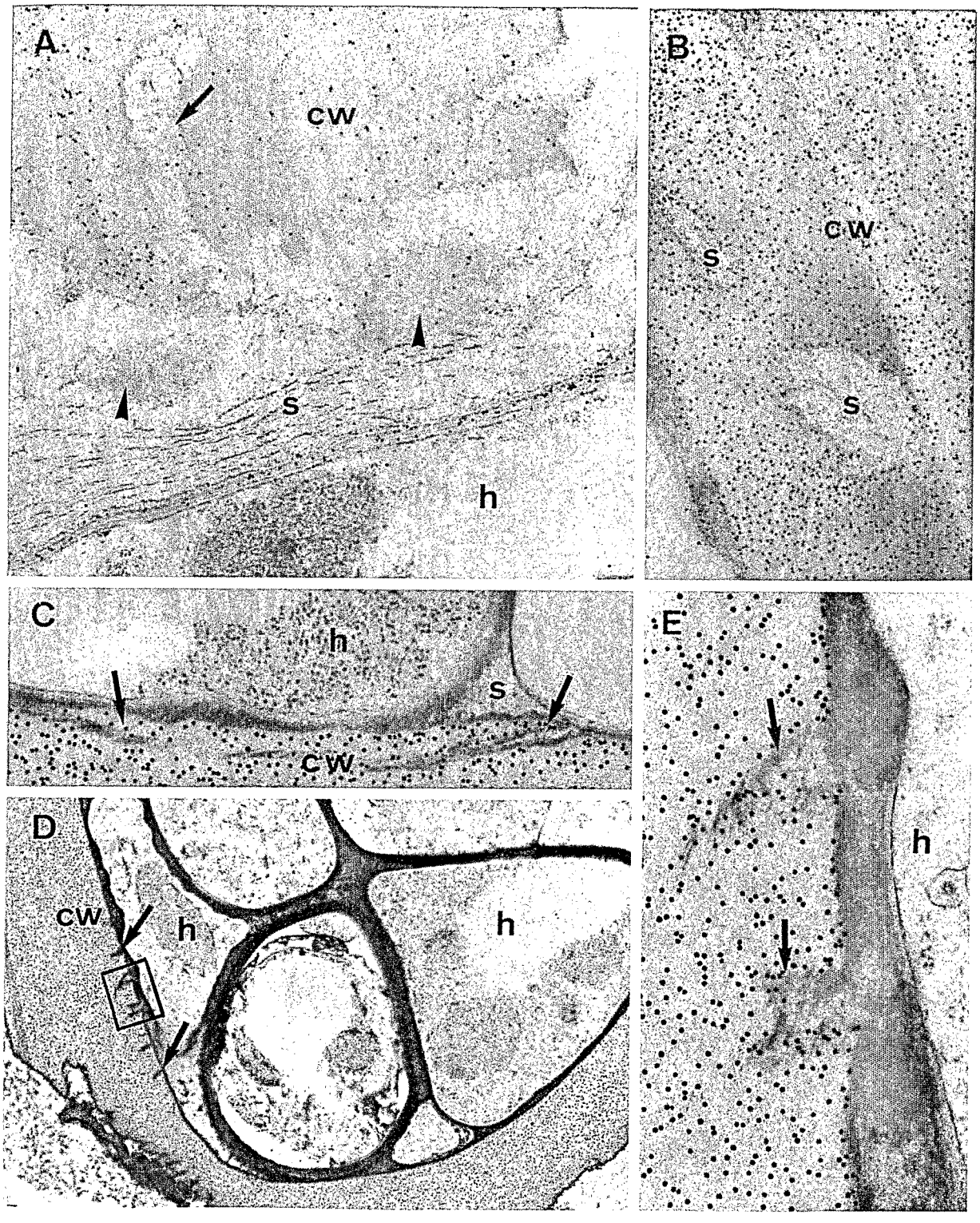

Fig. 6. TEM of wood degradation 6 days after inoculation with *P. noxius*. (A) Cytolocalization of *N*-acetylglucosamine residues. No gold particles are observed over the electron-dense fungal material (arrows), while the fungal cell wall is evenly labeled. × 28 000. (B) Hyphae observed within the cell walls are associated with wood alteration. Electron-dense material fills degraded wall areas (arrows), while fine dark granulation can be observed within eroded cell wall portions (arrowheads). × 35 000. (C) The electron-dense material (arrow) is associated with the fibrillar fungal sheath. × 32 000. (D) Cytolocalization of β-1,4-glucans in wood cell walls. In a transverse section, a microhypha is seen inside a secondary host cell wall. Wood degradation is observed in close contact with the fungus (arrows). × 38 000. (E) Cytolocalization of *N*-acetylglucosamine residues. Gold particles are distributed in a circle (arrow) within the wood cell wall, suggesting the occurrence of a fungal mycrohypha. The double arrow indicates a degraded area in the host cell wall. × 45 000. *h*, hypha; *cw*, wood cell wall; *m*, microhypha; *ml*, middle lamella; *s*, fungal sheath.

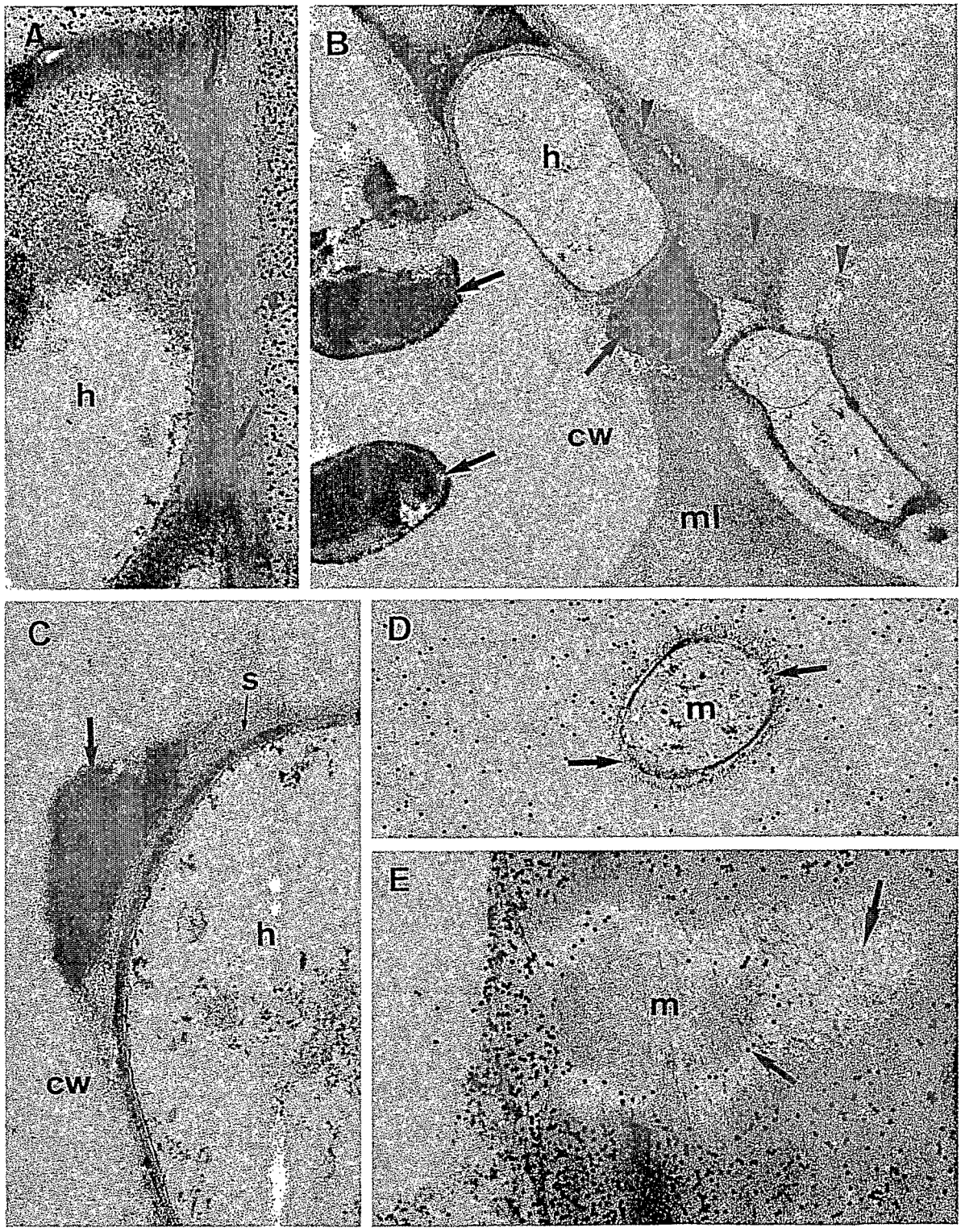

Fig. 7. TEM of wood degradation 11 days after inoculation with *P. noxius*. Cytolocalization of β-1,4-glucans in wood cell walls. (A) Residual labeled fragments are associated with degraded secondary wall (arrows). × 28 000. (B) Large fragments of degraded host walls are labeled. They are closely associated with the electron-dense fungal material and the thick-walled hypha. Few gold particles are localized within this dark material (arrows). Connections are seen between the fungal sheath and the thick-walled hypha (arrowhead). × 18 000. (C) A thick-walled hypha shows a multilayered organization with light and dark staining layers. Gold particles are seen within the extracellular fungal material (arrowheads). × 21 000. (D) The extracellular and electron-dense fungal material is closely associated with degraded areas of the wood secondary cell wall (arrows). × 37 500.

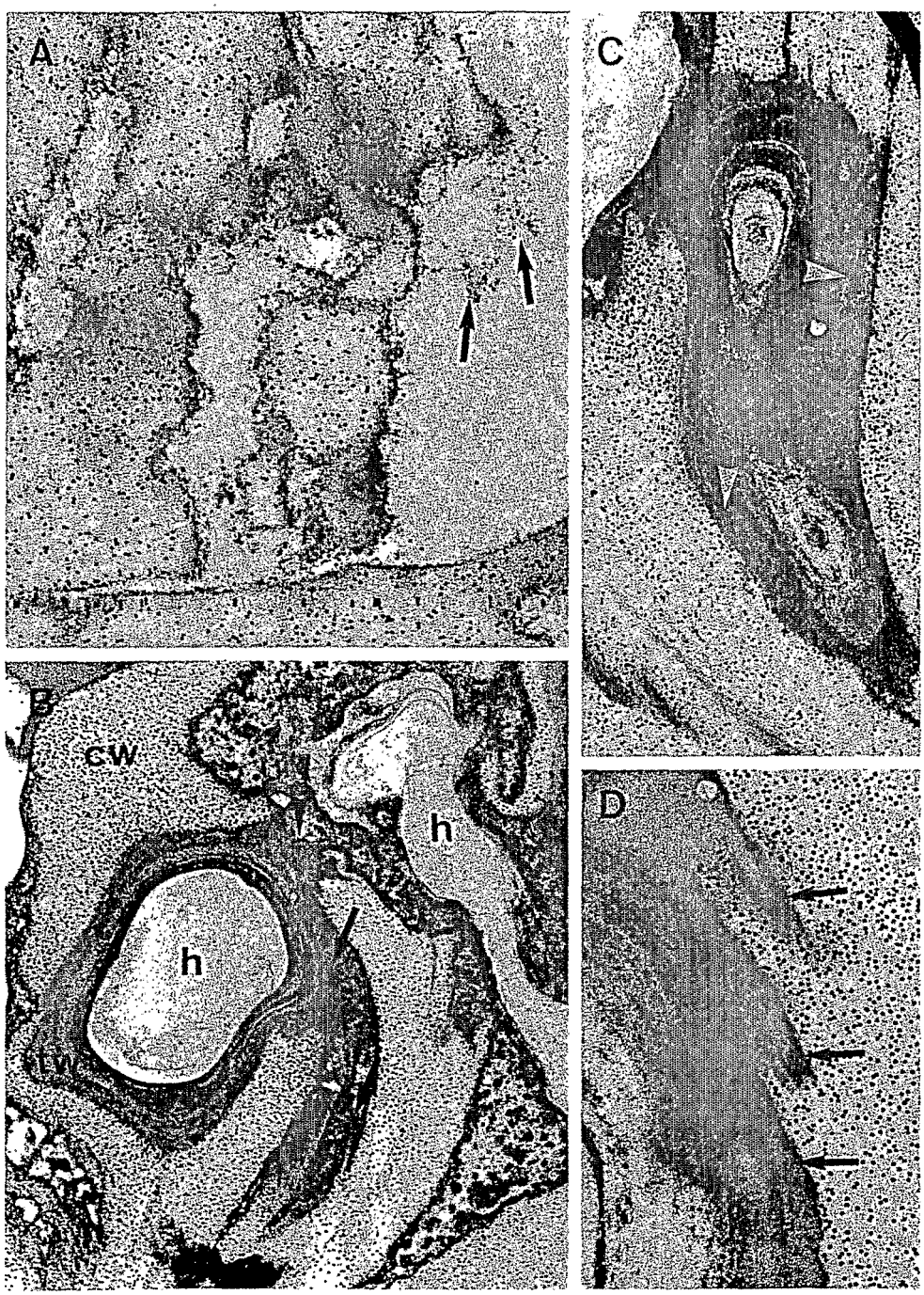

move within more or less lignified cell walls. Microhyphae were often surrounded by a halo that displayed various aspects of erosion at the margin of the cavity. Under our experimental conditions, the more abundant occurrence of microhyphae at an advanced stage of decay may be related to unfavorable environmental conditions that likely stimulated the production

of microhyphae that may act as conservation structures. Microhyphae would thus contribute to the fungal food supply, acting as nutrient channels following the release of wall-degrading enzymes (Highley et al. 1983).

Also, the increasing hyphal wall thickness in advanced stages of colonization might be related to unfavorable environmental conditions. It is likely that wall components such as phenolics are released from degraded wood and may become toxic to the fungus. Although *P. noxius* secretes detoxifying enzymes such as laccases (Geiger et al. 1986*b*, 1986*c*), the thick walls may act as a protective layer for the fungal cell. The extensive wall thickening likely results from both chitin and glucan synthesis. Chitin was shown, by gold labeling, to be evenly distributed within the thick walls; however, β-1,3-glucans, if present, were not accessible to the gold probe. Thick-walled hyphae have been described for some pathogens; in wood-degrading fungi, such hyphae occurred within rhizomorph strands (Schmid and Liese 1968) and were commonly observed at zone lines. *Rigidoporus lignosus*, another tropical root-rotting pathogen of rubber trees, displays hyphae with variable wall thickness in the rhizomorph. A considerable decrease in the wall thickness was observed when cells of *R. lignosus* hyphae became infecting structures (Nicole and Benhamou 1991*b*). In the absence of experimental studies, the significance of thick-walled hyphae in *P. noxius* wood decay remains unclear. However, the dark brown mycelial crust that covers roots after tree infection (Hodges 1984; Nandris et al. 1987) is always associated with plant infection.

In the present study, electron-opaque deposits were located in the fungal sheath several days after wood colonization. They are common features observed in advanced stages of decay. X-ray analysis did not reveal significant accumulation of manganese in *P. noxius* sheaths (data not shown). One may expect that these electron-opaque deposits may originate from melanin, since laccase is produced by *P. noxius* during infection (Geiger et al. 1986*b*, 1986*c*; Nicole et al. 1992) and was demonstrated to be involved in melanization (Faure et al. 1993). The role that melanin may play during wood biodegradation by *P. noxius* remains obscure, although it was demonstrated that melanization for some fungi may be an essential factor for successful penetration of host plants (Kubo and Furusawa 1991).

References

Adaskaveg, J.E., Gilbertson, R.L., and Blanchette, R.A. 1991. *Phellinus ralunenesis* (Aphyllophorales: Hymenochaetaceae), a new white pocket rot species from Chile. Mycol. Res. **95**: 769–775.

Bendayan, M. 1981. Ultrastructural localization of nucleic acids by the use of enzyme–gold complexes. J. Histochem. Cytochem. **29**: 531–541.

Bendayan, M., and Benhamou, N. 1987. Ultrastructural localization of glucoside residues on tissue sections by applying the enzyme–gold approach. J. Histochem. Cytochem. **35**: 1149–1155.

Benhamou, N., and Côté, F. 1992. Ultrastructure and cytochemistry of pectin and cellulose degradation in tobacco roots infected by *Phytophthora parasitica* var. *nicotianae*. Phytopathology, **82**: 468–478.

Benhamou, N., and Ouellette, G.B. 1987. Ultrastructural characterization of an extracellular sheath on cells of *Ascocalyx abietina*, the scleroderris canker agent of conifers. Can. J. Bot. **65**: 154–167.

Benhamou, N., Ouellette, G.B., Gardiner, R.B., and Day, A.W. 1986. Immunocytochemical localization of antigen-binding sites in the cell surface of two ascomycete fungi using antibodies produced against fimbriae from *Ustilago violacea* and *Rhodotorula rubra*. Can. J. Microbiol. **32**: 871–883.

Benhamou, N., Chamberland, H., Ouellette, G.B., and Pauze, F.J. 1987. Ultrastructural localization of β-(1,4)-glucans in two pathogenic fungi and their host tissues by means of an exoglucanase–gold complex. Can. J. Microbiol. **33**: 405–417.

Blanchette, R.A. 1980. Wood decomposition by *Phellinus (Fomes) pini*: a scanning electron microscopy study. Can. J. Bot. **58**: 1496–1503.

Blanchette, R.A. 1982. Decay and canker formation by *Phellinus pini* in white and balsam fir. Can. J. For. Res. **12**: 538–544.

Blanchette, R.A., Abad, A.R., Farrell, R.L., and Leathers, T.D. 1989. Detection of lignin peroxidase and xylanase by immunocytochemical labeling in wood decayed by Basidiomycetes. Appl. Environ. Microbiol. **55**: 1457–1465.

Corbett, N.H. 1965. Micro-morphological studies on the degradation of lignified cell walls by Ascomycetes and Fungi Imperfecti. Inst. Wood Sci. J. **3**: 18–29.

Faure, D., Bouillant, M.L., and Bally, R. 1993. Isolement de mutants Tn*5* deficients pour l'activité laccase et la production de melanine chez *Azospirillum lipoferum*. *In* Abstracts of the 3rd Annual Meeting of the Société Française de Phytopathologie, Dijon, France, 1993. Abstr. p-184.

Frens, G. 1973. Controlled nucleation for regulation of the particle size in monodisperse gold suspensions. Nat. Phys. Sci. **241**: 20–22.

Gallagher, M.I., and Evans, C.S. 1990. Immunogold-cytochemical labelling of β-glucosidase in the white-rot fungus *Coriolus versicolor*. Appl. Microbiol. Biotechnol. **32**: 588–593.

Geiger, J.P., Nicole, M., Nandris, D., and Rio, B. 1986*a*. Root rot diseases of *Hevea brasiliensis*. I. Physiological and biochemical aspects of root aggression. Eur. J. For. Pathol. **16**: 22–36.

Gieger, J.P., Rio, B., Nicole, M., and Nandris, D. 1986*b*. Biodegradation of *Hevea brasiliensis* wood by *Rigidoporus lignosus* and *Phellinus noxius*. Eur. J. For. Pathol. **16**: 147–159.

Geiger, J.P., Rio, B., Nandris, D., and Nicole, M. 1986*c*. Laccases of *Rigidoporus lignosus* and *Phellinus noxius*. I. Purification and some physico-chemical properties. Appl. Biochem. Biotechnol. **12**: 121–133.

Green, F., III, Clausen, C.A., Larsen, M.J., and Highley, T.L. 1992. Immuno-scanning electron microscopic localization of extracellular wood-degrading enzymes within the fibrillar sheath of the brown-rot fungus *Postia placenta*. Can. J. Microbiol. **38**: 898–904.

Hale, M.D., and Eaton, R.A. 1985*a*. Oscillatory growth of fungal hyphae in wood cell walls. Trans. Br. Mycol. Soc. **84**: 277–288.

Hale, M.D., and Eaton, R.A. 1985*b*. The ultrastructure of soft rot fungi. I. Fine hyphae in wood cell walls. Mycologia, **77**: 447–463.

Hale, M.D., and Eaton, R.A. 1985*c*. The ultrastructure of soft rot fungi. II. Cavity-forming hyphae in wood cell walls. Mycologia, **77**: 594–605.

Highley, T.L., Palmer, J.G., and Murmanis, L.L. 1983. Decomposition of cellulose by *Poria placenta*: light and electron microscopy study. Holzforschung, **37**: 179–184.

Hodges, C.S. 1984. Root disease of *Delonix regia* and associated tree species in the Mariana islands caused by *Phellinus noxius*. Plant Dis. **68**: 334–336.

Knox, J.P., Linstead, P.J., King, J., Cooper, C., and Roberts, K. 1990. Pectin esterification is spatially regulated both within cell walls and between developing tissues of root apices. Planta, **181**: 512–521.

Kubo, Y., and Furusawa, I. 1991. Melanin biosynthesis. Prerequisite for successful invasion of the plant host by appressoria of *Colletotrichum* and *Pyricularia*. *In* The fungal spore and disease initiation in plants and animals. *Edited by* G. Tole and H. Hoch. Plenum Press, New York. pp. 205–218.

Liese, W., and Schmid, R. 1963. Fibrilläre Strukturen an dem Hyphen holzzerstörender Pilze. Naturwissenschaften, **50**: 102–103.

Murmanis, L., Highley, T.L., and Palmer, J.G. 1984. An electron microscopy study of western hemlock degradation by the white-rot fungus *Ganoderma applanatum*. Holzforschung, **38**: 11–18.

Nandris, D., Nicole, M., and Geiger, J.P. 1987. Root rot diseases of rubber tree. Plant Dis. **71**: 298–306.

Nicole, M., and Benhamou, N. 1991*a*. Cytochemical aspects of cellulose breakdown during the infection process of rubber tree roots by *Rigidoporus lignosus*. Phytopathology, **81**: 1412–1420.

Nicole, M., and Benhamou, N. 1991*b*. Ultrastructural localization of chitin in cell walls of *Rigidoporus lignosus*, the white-rot fungus of rubber trees. Physiol. Mol. Plant Pathol. **39**: 415–432.

Nicole, M., Geiger, J.P., and Nandris, D. 1987. Ultrastructural aspects of rubber tree root rot diseases. Eur. J. For. Pathol. **17**: 1–10.

Nicole, M., Chamberland, H., Geiger, J.P., Lecours, N., Valéro, J., Rio., B., and Ouellette, G.B. 1992. Immunocytochemical localization of laccase L1 in wood decayed by *Rigidoporus lignosus*. Appl. Environ. Microbiol. **58**: 1727–1739.

Nicole, M., Chamberland, H., Rioux, D., Geiger, J.P., Rio, B., Lecours, N., and Ouellette, G.B. 1993. A cytochemical study of extracellular sheaths associated to *Rigidoporus lignosus* during wood decay. Appl. Environ. Microbiol. **59**: 2578–2588.

Nicole, M., Ruel, K., and Ouellette, G.B. 1994. Fine morphology of fungal structures involved in host cell wall alterations. *In* Host wall alteration by parasitic fungi. *Edited by* O. Petrini and G.B. Ouellette. APS Press, St. Paul, Minn. pp. 13–31.

Ouellette, G.B. 1962. Morphological characteristics of *Ceratocystis ulmi* (Buism.) C. Moreau in American elm trees. Can. J. Bot. **40**: 1463–1466.

Peek, R.D., Liese, W., and Parameswaran, N. 1972. Infektion und Abbau der Wurzelrinde von Fichte durch *Fomes annosus*. Eur. J. For. Pathol. **2**: 104–115.

Roth, J. 1983. Application of lectin–gold complexes for electron microscopic localization of glycoconjugates on thin sections. J. Histochem. Cytochem. **31**: 987–997.

Roth, J., Lucocq, J.M., and Charest, P.M. 1984. Light and electron microscopic demonstration of sialic acid residues with the lectin from *Limax flavus*: a cytochemical affinity technique with the use of fetuin-gold complexes. J. Histochem. Cytochem. **32**: 1167–1176.

Ruel, K., and Joseleau, J.P. 1991. Involvement of an extracellular glucan sheath during degradation of *Populus* wood by *Phanerochaete chrysosporium*. Appl. Environ. Microbiol. **57**: 374–384.

Schmid, R., and Liese, W. 1968. Structural and histochemical observations on fungal finer hyphae. *In* Electron microscopy. Vol. 2. *Edited by* D.S. Boccarielli. Tipographia Pologlotta Vaticana, Rome, Italy. p. 415.

Thiéry, J.-P. 1967. Mise en évidence des polysaccharides sur coupes fines en microscopie électronique. J. Microsc. Paris, **6**: 987–1018.

Thrower, L.B. 1965. Parasitism of cocoa by *Fomes noxius* in Papua-New Guinea. Top. Agric. Trin. **42**: 63–67.

Wessels, J.G.W., and Sietsma, J.H. 1981. Fungal cell walls: a survey. *In* Plant carbohydrates. II. *Edited by* W. Tanner and Loewers. Springer Verlag, New York. pp. 352–394.

Zainal, A.S. 1976. The soft rot fungi: the effect of lignin. Beih. Mat. Org. No. 3. pp. 21–127.